JOURNAL OF GEOPHYSICAL RESEARCH, VOL. 112, D15307, doi:10.1029/2007JD008618, 2007

Aerosol and fresh snow chemistry in the East Rongbuk Glacier on the northern slope of Mt. Qomolangma (Everest)

Jing Ming,[1,2,3] Dongqi Zhang,[2,3] Shichang Kang,[4] and Wanshun Tian[5]

Received 6 March 2007; revised 23 April 2007; accepted 8 May 2007; published 11 August 2007.

[1] An intensive and simultaneous sampling for aerosol and fresh snow was conducted at Repula Col of the East Rongbuk Glacier near Mt. Qomolangma during the late Indian summer monsoon season in 2003. Aerosol and snow chemistry (including the species of Na^+, K^+, Mg^{2+}, Ca^{2+}, Cl^-, SO_4^{2-}, and NO_3^-) is analyzed and discussed. Anions account for a majority of the air quality, and SO_4^{2-} is the most loaded species. Local emission by land weathering does not contribute significantly to the loading of Mg^{2+} and Ca^{2+}, and their high concentration is related to their continental desert sources. The meridional dynamic force of Indian monsoon is efficient to the loading of Na^+, and Na^+/Ca^{2+} could be used to distinguish air masses of maritime or continental which dominate the air quality. The signal of crustal SO_4^{2-} from Central/West Asia or farther Africa is weak, and mixed sources (anthropogenic and crustal) of SO_4^{2-} dominate its loading in aerosol samples. Air–snow scavenging ratios of these species are calculated and compared with the other results in some previous studies. The scavenging ratio of SO_4^{2-} as the most heavily loaded species is around 200, which is comparable with that in Greenland.

Citation: Ming, J., D. Zhang, S. Kang, and W. Tian (2007), Aerosol and fresh snow chemistry in the East Rongbuk Glacier on the northern slope of Mt. Qomolangma (Everest), *J. Geophys. Res.*, *112*, D15307, doi:10.1029/2007JD008618.

1. Introduction

[2] The extensive Himalayan range stretches about 2500 km from west to east along the southern margin of the Tibetan Plateau, thereby forming a barrier between tropical and polar air masses [*Nieuwolt*, 1977]. During the winter, the Himalayas and Tibetan Plateau deflect strong westerly winds along their northern and southern margins, while in summer, the Himalayas restrict the penetration of southeasterly monsoon air masses into the interior regions of the Plateau. In this case, the Himalayas and the Tibetan Plateau play an important role in regional scale atmospheric circulation patterns over Asia. Mt. Qomolangma region, located on the central Himalayas with an average elevation over 5000 m a.s.l., spans the middle and top layers of troposphere, and in addition, it is far away from heavily industrialized areas (e.g., South Asia, East Asia). Looking from the north, this region faces fast developing South Asia with massive emission every year [e.g., *Ramanathan et al.*, 2001; *Venkataraman et al.*, 2005] and at its back is the relatively cleaner Tibetan Plateau and thus provides an ideal environment for the study of atmospheric chemistry of species of long-range transported from South Asia during summer monsoon season.

[3] Glaciochemical records have been proven to be an excellent tool to investigate the atmospheric composition of the past [e.g., *Mayewski et al.*, 1983, 1990; *Wake et al.*, 1990; *Legrand and Mayewski*, 1997]. The glaciochemical records contained in the glaciers near Mt. Qomolangma present a valuable resource to document the information of atmospheric deposition in this region and to reconstruct the history of past regional climatic and environmental change [e.g., *Qin et al.*, 2000, 2002; *Zhang et al.*, 2005]. And during the past few years, a number of work on the ice cores drilled here have been carried out [e.g., *Kang et al.*, 2001a, 2001b, 2002a, 2002b; *Hou et al.*, 2003] to investigate the nature of glaciochemical variations of long-timescale in the nearby glaciers. Furthermore, fresh and surface snow chemistry was also studied here to understand seasonal changes of atmospheric deposition [e.g., *Valsecchi et al.*, 1999; *Marinoni et al.*, 2001; *Kang et al.*, 2004]. In general, these studies approached to investigate variations of atmospheric composition using snow chemistry.

[4] However, the quantitative estimate of the past atmospheric chemical composition based on glaciochemical data depends greatly on the knowledge of the relationship between chemical amounts of fresh snow and aerosol. However, their relationship is specific at different sites [e.g., *Davidson et al.*, 1985, 1993; *Silvente and Legrand*, 1993; *Baltensperger et al.*, 1993; *Sun et al.*, 1998; *Shrestha et al.*, 2002]. Understanding the chemical composition of the atmosphere near Mt. Qomolangma, its temporal and spatial variability, and the relationships between the com-

[1]Institute of Geology and Geophysics, Chinese Academy of Sciences, Beijing, China.
[2]Institute of Climate System, Chinese Academy of Meteorological Sciences, Beijing, China.
[3]State Key Laboratory of Cryospheric Sciences, Lanzhou, China.
[4]Institute of Tibetan Plateau Research, Chinese Academy of Sciences, Beijing, China.
[5]Zhengzhou Weather Modification Center, Chinese Meteorological Administration, Zhengzhou, China.

0148-0227/07/2007JD008618$09.00

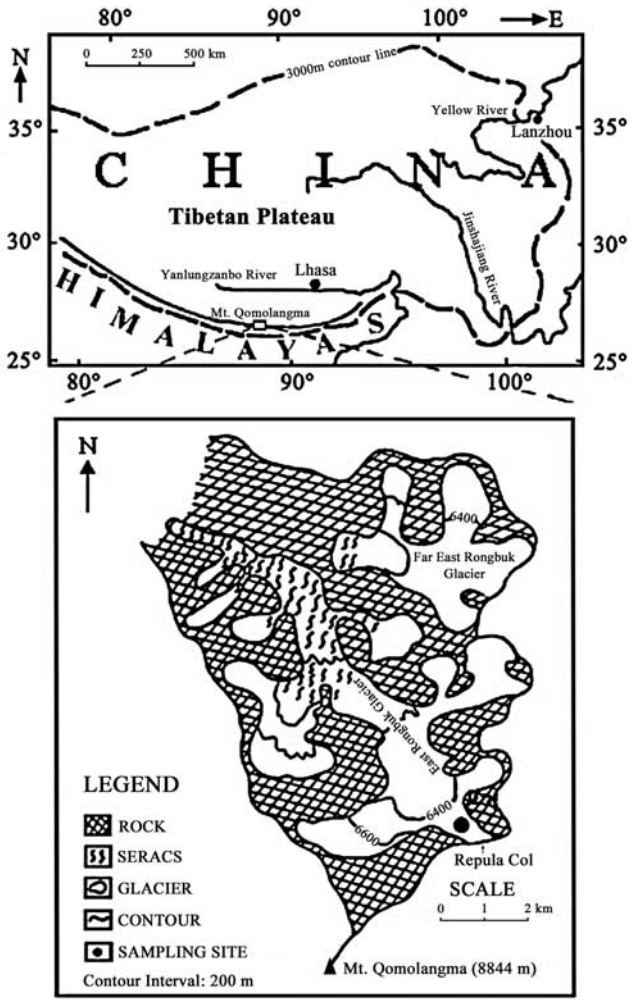

Figure 1. Location map of the sampling site at the Repula Col of the East Rongbuk glacier, Mt. Qomolangma.

positions of the snow and air are very essential for an improved interpretation of the glaciochemical records. Hence the simultaneous sampling experiment of aerosol and fresh snow is indeed needed in here.

[5] Due to the atrocious transport condition and working environment near Mt. Qomolangma, studies on atmospheric chemistry have been very limited to date on both temporal and spatial scales. A short-term sampling program in the Nguzompa glacier basin near Mt. Qomolangma showed low ion burdens in both aerosol and snow [*Wake et al.*, 1994a, 1994b]. A 1-year-long sampling of atmospheric aerosol and precipitation was conducted at Phortse [*Shrestha et al.*, 2000, 2002]. Above two studies were both accomplished on the southern slope of Mt. Qomolangma, while no data on aerosol chemistry are reported on the northern slope of Mt. Qomolangma up to now.

[6] From 10 to 25 September 2003, an intensive and simultaneous sampling experiment for aerosol and fresh snow and a meteorological observation were conducted at Repula Col of the East Rongbuk Glacier on the northern slope of Mt. Qomolangma. The purpose of this study is to obtain an updated knowledge of aerosol composition here and to improve the interpretation for the glaciochemical records. The intensive sampling for 16 days will help to understand the temporal variability of aerosol composition during the late summer monsoon season. The meteorological observation is necessary for investigating the response of air species to local crustal dust caused by weathering. Air–snow relationship here was attempted to be investigated for the first time. Although the field experiment covered only 16 days, this study is the most detailed one of such works achieved on the northern slope of Mt. Qomolangma by now.

2. Site Description

[7] The sampling site (28.02°N, 86.96°E, 6500 m a.s.l.) is located at Repula Col of the East Rongbuk Glacier (Figure 1). East Rongbuk Glacier is surrounded by mountains ranging from 6000 m to over 8000 m a.s.l. including Mt. Qomolangma (8844 m a.s.l.). An easier accessible pathway for moist air masses carried by the Indian monsoon arriving at East Rongbuk Glacier is Repula Col, located at the northeast saddle of Mt. Qomolangma. Figure 2 depicts the mean wind field (based on the National Centers for Environmental Prediction/National Center for Atmospheric Research [NCEP/NCAR] reanalysis data) at the geopotential height level of 500 hPa, covering the sampling period. Apparently southeast and southwest winds dominate the investigating area during the sampling period.

3. Experimental Methods

3.1. Aerosol Sampling

[8] Zefluor™ Teflon filters with 2-μm pore size, 47-mm diameter (Gelman Sciences) were mounted in a protective polyethylene cover. Five of the filters were used as field blanks and enveloped in the box. The air was sucked by a 12-V pump powered by a combination of solar cells and storage batteries. The volume of air sampled was measured by an in-line flowmeter. Corrections for ambient temperature and pressure allowed conversion of the measured volumes to standard cubic meters (in brief "scm"). The volume averages 12.02 scm for aerosol samplings.

[9] The mean flow rate was 0.4 scm h^{-1}, yielding a velocity at the face of the filter of 6.57 cm s^{-1}, which was high enough so that the efficiency of collection for particles as small as 0.3 μm is >99% [*Liu et al.*, 1984].

[10] Filters were loaded in the field and mounted face down about 1.5 m above the snow surface. When loading or unloading the filters, the operator wore plastic gloves and faced upwind in order to minimize contamination. After each sampling, the filter was removed from the filter cover and put into a pre-cleaned airtight plastic container. Aggregately, 12 filters loaded with aerosol samples were collected in the field during the sampling period. And both sample and field blank filters were stored at 4 °C from field to laboratory before analyzing in the State Key Laboratory of Cryospheric Sciences, Chinese Academy of Sciences (Lanzhou).

[11] In the clean room of 100 class, all sample and field blank filters were carefully moved into the pre-cleaned tubes, mixed with 200 μl ethanol, diluted with 20 ml

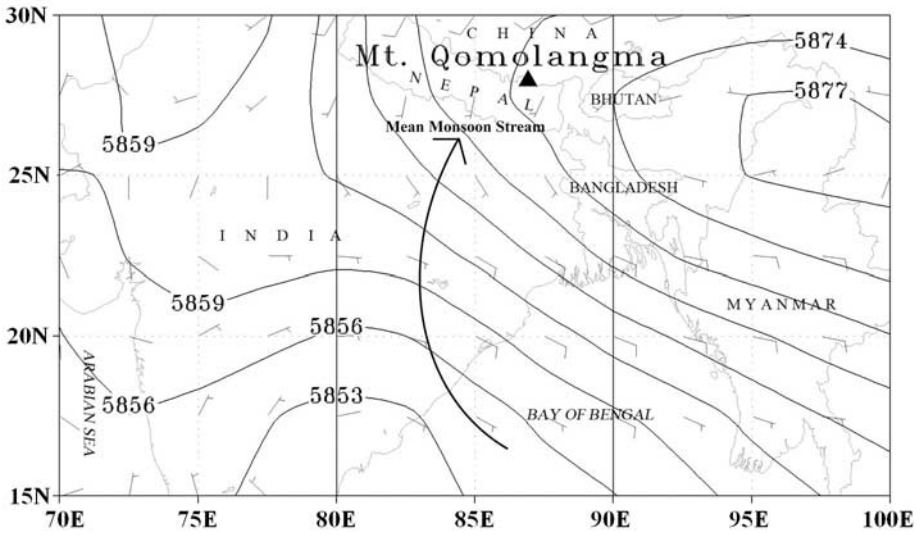

Figure 2. The average wind field in the area of 70–100°E and 15–30°N, from 10 to 25 September 2003.

Milli-Q water (18.2 Ω), and extracted for about 1 hour using an ultrasonic water bath device. After that, a pre-cleaned glass bar was used to stir the filters in the tubes in order to make the extraction completely. And then the extraction in the water bath with an ultrasonic device process was carried through again for another hour. At last, the tubes were moved into a refrigerator and kept for 12 hours at a temperature of 4 °C.

[12] Seven ions (Na^+, K^+, Mg^{2+}, Ca^{2+}, Cl^-, SO_4^{2-}, and NO_3^-) in the aerosol samples were analyzed using a Dionex™ model 600 ion chromatography. The chromatography conditions were as follows: for cations, CS12 analytical column, 22 mM methanesulfonic acid (MSA) eluent, cation self-regenerating suppressor and 800 μl sample loop; for anions, AS11 analytical column, 12 mM NaOH eluent, anion self-regenerating suppressor and 800 μl sample loop.

[13] Mean concentrations of five field blank filters were (in μeq l^{-1}): Na^+ (0.15), K^+ (0.02), Mg^{2+} (0.02), Ca^{2+} (3.34), Cl^- (0.01), SO_4^{2-} (0.03), and NO_3^- (0.02), which were 6–350 times lower than the average concentration measured in aerosol samples. Mean field blank values were subtracted from the sample values.

3.2. Fresh Snow Sampling

[14] During the sampling period, five fresh snow samples were collected during the 16-day sampling. Each sample was collected within 24 hours after the end of each snow event at the downwind snow surface 2 m away from the aerosol sampling site. Snow samples were collected in plastic bags using a plastic scraper. The samples were melted in the field, transferred into pre-cleaned containers, and transported to the State Key Laboratory of Cryospheric Sciences, Chinese Academy of Sciences (Lanzhou), where they were refrozen for storage. Seven ions same as those in the aerosol filters in snow samples were also measured using the Dionex™ model 600 ion chromatography.

3.3. Meteorological Data

[15] An automatic weather station (AWS, Vantage Pro Plus®, Davis Company, and USA) was set up beside the aerosol sampling site. Its power system made of solar cells and storage batteries can guarantee AWS to keep working in a 24-hour mode. Local wind speed and direction were recorded every 15 minutes. The AWS kept working from 10 to 25 September 2003.

4. Results and Discussion

4.1. Overview

[16] To provide a general indication of the chemical characteristics of the aerosol samples, a summary of equivalent concentration for the seven ions measured (Na^+, K^+, Mg^{2+}, Ca^{2+}, Cl^-, SO_4^{2-}, and NO_3^-) in aerosol samples is presented in Table 1. Some items of interest are also calculated; for example, weighted average (on standard air flux of each filter) concentration, sharing percentage, and minimum and maximum of each species are given out. We also calculated

$$\Sigma^+ = [Na^+] + [K^+] + [Mg^{2+}] + [Ca^{2+}],$$

$$\Sigma^- = [Cl^-] + [SO_4^{2-}] + [NO_3^-],$$

$$\Sigma^+ + \Sigma^- = ([Na^+] + [K^+] + [Mg^{2+}] + [Ca^{2+}]) + ([Cl^-] + [SO_4^{2-}] + [NO_3^-]),$$

$$\Sigma^+ - \Sigma^- = ([Na^+] + [K^+] + [Mg^{2+}] + [Ca^{2+}]) - ([Cl^-] + [SO_4^{2-}] + [NO_3^-]).$$

[17] Anions dominate the aerosol composition during the sampling period. Mean Σ^- is almost three times as much as mean Σ^+, and comparing the two columns of Σ^+ and Σ^- in Table 1, the values of ($\Sigma^+ - \Sigma^-$) in most samples are negative, except that on 22/23. Among seven ions, SO_4^{2-} is the most loaded species on filters, whose mean concentra-

Table 1. Concentrations of the Species and Some Items of Interest

Date (b/e)	Na^+	K^+	Mg^{2+}	Ca^{2+}	Cl^-	SO_4^{2-}	NO_3^-	Σ^+	Σ^-	$\Sigma^+ + \Sigma^-$	$\Sigma^+ - \Sigma^-$
10/12	0.18	0.11	2.44	3.48	0.79	7.06	0.50	6.21	8.35	14.56	−2.14
12/14	0.07	0.25	0.98	1.98	1.10	6.59	0.85	3.28	8.54	11.82	−5.26
14/15	3.90	1.06	1.30	3.39	1.78	12.79	4.47	9.65	19.04	28.69	−9.39
15/16	0.37	0.93	0.66	1.61	2.42	10.23	3.31	3.57	15.96	19.53	−12.39
16/17	2.44	0.33	0.33	0.23	3.98	9.94	3.70	3.33	17.62	20.95	−14.29
17/18	2.30	1.05	0.31	0.37	1.42	4.13	2.01	4.03	7.56	11.59	−3.53
18/19	1.10	0.40	0.41	0.16	1.35	22.20	4.14	2.07	27.69	29.76	−25.62
19/20	0.28	0.22	0.17	0.39	1.90	4.55	2.45	1.06	8.90	9.96	−7.84
20/22	0.65	0.18	0.79	3.73	8.49	12.84	4.84	5.35	26.17	31.52	−20.82
22/23	4.73	1.03	1.88	4.65	2.53	4.92	1.07	12.29	8.52	20.81	3.77
23/24	2.15	0.30	0.76	1.43	2.63	3.16	0.00	4.64	5.79	10.43	−1.15
24/25	4.54	0.61	0.77	0.14	4.23	2.61	0.99	6.06	7.83	13.89	−1.77
Weighted. Ave.	1.39	0.43	0.98	2.00	2.80	8.58	2.29	4.80	13.66	18.47	−8.86
Sharing %	7.55	2.34	5.30	10.83	15.15	46.44	12.40	26.02	73.98		−47.97
Min.	0.07	0.11	0.17	0.14	0.79	2.61	0.00	1.06	5.79	9.96	−25.62
Max.	4.73	1.06	2.44	4.65	8.49	22.20	4.84	12.29	27.69	31.52	3.77
|Max./Min.|	67.57	9.64	14.35	33.21	10.75	8.51	9.68	11.59	4.78	3.16	0.15
SD	1.73	0.38	0.68	1.63	2.11	5.61	1.69	3.17	7.63	7.86	8.63

"b/e" Stands for "beginning/end" time of each sampling; "Wtd. Ave." stands for weighted average of each ion concentration; "Sharing %" stands for mean sharing percentage of each ion in Σ^+.

tion accounts for nearly a half of mean ($\Sigma^+ + \Sigma^-$). And the next places are Cl^-, NO_3^-, Ca^{2+}, Na^+, Mg^{2+}, and K^+, respectively.

[18] The quotients of maximum and minimum mean concentration of the ions (Max./Min.) are used to describe varying amplitudes of each species. In general, the variability of cations is much bigger than that of anions. Na^+ has the biggest variability (Max./Min. = 67) among the ions; Ca^{2+} takes the second place (Max./Min.=33); and their variability exceeds that of other ions by times. Anions (Cl^-, SO_4^{2-}, and NO_3^-) have similar Max./Min., and no significant variability could be distinguished through the Max./Min. values of them.

4.2. Daily Variations and Transport of Aerosols and Their Relationship With Meteorological Condition

4.2.1. Interspecies Relationships and Grouping of Ions

[19] Correlation coefficients among the seven ions are calculated, and three couples of ions with closer relationships are obtained, which are Na^+-K^+ (0.615, $\alpha = 0.05$), Mg^{2+}-Ca^{2+} (0.797, $\alpha = 0.01$), and NO_3^--SO_4^{2-} (0.765, $\alpha = 0.01$), respectively. A more detailed description of the daily concentration variations of the seven ions is presented in Figure 3 (step plots), in which each step begins at the beginning and ends at the end of each sampling.

[20] Based on the correlation coefficients between the species and similarities of general varying trends of them showed in Figure 3, four groups of ions could be distinguished. Table 2 presents a tabulation of the peak-showing time of these species belonging to the four groups, respectively. The peak value is defined as one of the following three rules; that is, (1) the line of the assumed peak value in Figure 3 must be above the weighted average line (dashed line in Figure 3) of the related species; (2) if there are adjacent high values, the assumed peak value must be the highest one; (3) the discrepancy of the assumed peak value and its former proximate value must exceed or be close to the standard deviation of the related species concentration. Thus Na^+ and K^+ show their simultaneous peaks on 14/15, 22/23, and 24/25; Mg^{2+} and Ca^{2+} show three simultaneous peaks on 10/12, 14/15, and 22/23; SO_4^{2-} and NO_3^- also show three simultaneous peaks on 14/15, 18/19, and 20/22; Cl^- is a single and special species and it shows a significant peak on 20/22, and on 16/17 and 24/25, it shows two mild concentration pulses.

4.2.2. Loading of Some Selected Species and Their Relationship With the Transport

[21] Backward trajectory analysis has been applied widely in the field of atmospheric sciences [e.g., *Kahl et al.*, 1997]. And the Hybrid Single-Particle Lagrangian Integrated Trajectory (HYSPLIT) model (http://www.arl.noaa.gov/ready/hysplit4.html, NOAA Air Resources Laboratory) is one of the valid tools to model the air trajectory among the models and has been credibly used in some previous studies [e.g., *Falkovich et al.*, 2001; *Ramachandran*, 2005; *Marenco et al.*, 2006]. The global estimate of the average lifetime of sulfate aerosol is about 5 days [*Langner and Rodhe*, 1991], and during Indian Ocean Experiment (INDOEX), the aerosol lifetime over the INDOEX field was estimated to be 7 to 8 days [*Rasch et al.*, 2001]. Thus we use a compromised method of 6-day-long backward trajectory with a daily resolution to simulate the moving routes of air masses arriving at the sampling site after setting our ending location at the sampling site (28.02°N, 86.96°E, 6500 m a.s.l.) and ending time at 12:00 (04:00 UTC) of Beijing time in the middle of each day. The results of backward trajectory analysis are presented in Figure 4. The air masses arriving at our sampling site are generally travelling from four directions, which are Central/West Asia and farther Africa of long-distance transport, Thar Desert area, Bay of Bengal, and Southeast Asia, respectively. To obtain more detailed information of air masses transported and to investigate their relationship with the different performances of the aerosol species on the filters, Figure 5 is presented. Among these trajectories, the two ending on the 22nd and 23rd are the most distinct. They suggest the sample loaded on the filter of 22/23 carried by westerly travelled a very long distance from West Africa, even from much farther places suggested by their vertical moving profiles. These two trajectories steer clear of the heavily contaminated Ganga

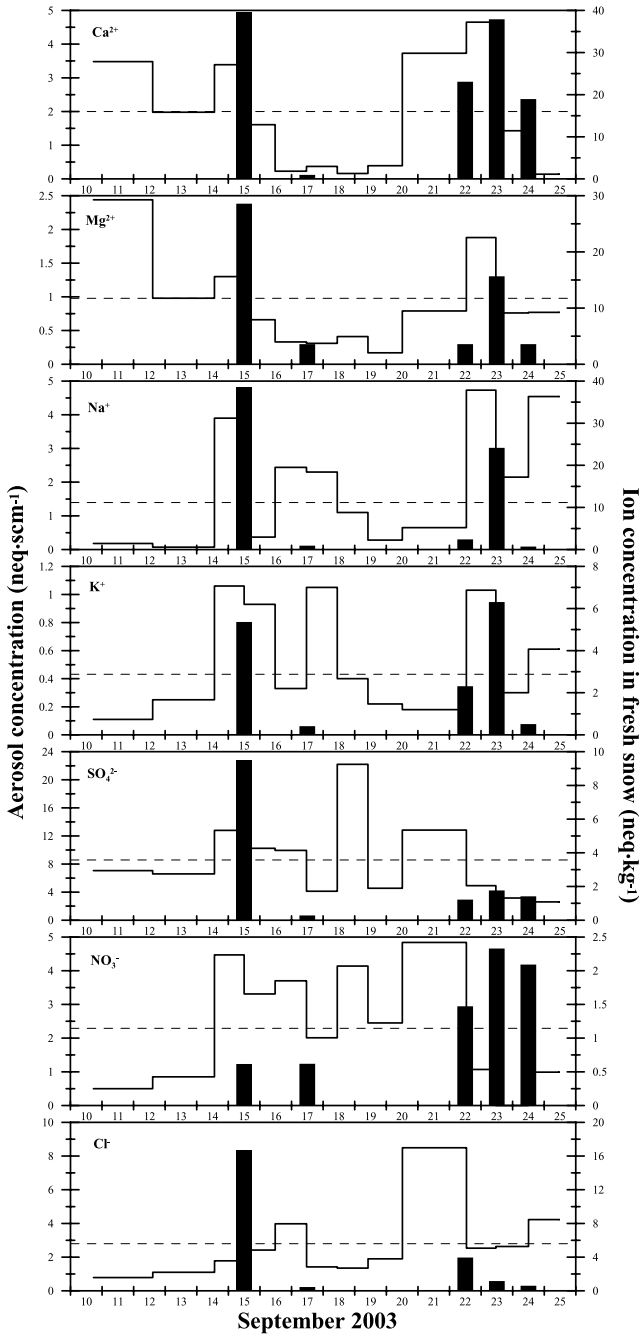

Figure 3. Concentration of major ions in aerosol (step plots) and in fresh snow samples (black bars).

basin [e.g., *Goloub et al.*, 2001; *Singh et al.*, 2004] and arrive here, thus might result in the unique positive value (3.77) of ($\Sigma^+ - \Sigma^-$) showed in Table 1.

[22] As shown in Figure 2, the mean wind field of the sampling period suggests that the air masses arriving at the sampling site are dominantly controlled by the southerly winds. The concentration plots of most species (Na^+, K^+, Cl^-, SO_4^{2-}, and NO_3^-) in Figure 3 show similar "M" varying patterns, whereas the variability of Mg^{2+} and Ca^{2+} shows a "U" valley during our sampling period. Why does the group of Mg^{2+} and Ca^{2+} present so special a group among the four groups of ions? Ca^{2+} and Mg^{2+} were thought to have crustal sources in the previous studies on snow and ice chemistry carried out near Mt. Qomolangma [e.g., *Wake et al.*, 1994b; *Kang et al.*, 2001a; *Kang et al.*, 2002a; *Kang et al.*, 2004]. Questions that local crustal emission might contribute some loading to the filters due to the rocky land weathering nearby caused by the local wind may be raised. Figure 6 presents the records of the AWS for local wind speed and direction. In most time of the experiment, local wind direction is southeasterly, suggesting that the wind field in the surface layer of our sampling site is consistent with the synoptic condition of the larger scale showed in Figure 2. We preclude the possibility of local crustal emission of Ca^{2+} or Mg^{2+} after considering poor loading of Ca^{2+} and Mg^{2+} for each sample (Table 1) and comparing the local wind speed with the concentration of Ca^{2+} or Mg^{2+} shown in Figure 3. The variability of Mg^{2+} and Ca^{2+} seems to be very sensitive to the air trajectories sourced from the dry desert areas. For example, the trajectories ending on 10, 11, 12, and 15 are sourced from Thar Desert area, and those ending on 22 and 23 are from farther West Africa. In the filters collected on 10/12, 14/15, and 22/23, we obtain three peak concentrations for the group of Mg^{2+} and Ca^{2+} (Figure 3). While in the other samples, Mg^{2+} and Ca^{2+} keep low concentration in relevant time periods. Thereby, the desert areas, Thar Desert, and Central/West Asia or farther Africa contribute significantly to the loading of Mg^{2+} and Ca^{2+} in our filters.

[23] Vertical profiles of the back trajectories in Figure 5 show that, in most cases, air masses travel roughly as a quasi-isobaric moving pattern between the isobaric layers of 600 and 700 hPa before their apparent ascend in Nepal mountain regions except those on 22nd and 23rd. And the heights of these trajectories are generally above the planet boundary layer and almost in the free troposphere over South Asia. Figure 2 suggests that wind field in the square area of 15–30°N, 80–90°E has the most significant impact (compared with the other areas) on the dynamic pattern of the air masses arriving at the sampling site during the experiment. Daily area-averaged meridional wind speed of the isobaric layers of 600 and 700 hPa in this square area are calculated based on the NCEP/NCAR Reanalysis daily V-wind data and showed in Figure 7, in which Na^+ concentration plot is also included. The concentration variation of Na^+ has a co-variation trend with the meridional wind speed

Table 2. Peak-Showing Time of the Species

Date (b/e)	Na^+	K^+	Mg^{2+}	Ca^{2+}	SO_4^{2-}	NO_3^-	Cl^-
10/12			×	×			
12/14							
14/15	×	×	×	×	×	×	
15/16							
16/17	×						×
17/18		×					
18/19					×	×	
19/20							
20/22					×	×	×
22/23	×	×	×	×			
23/24							
24/25	×	×					×

"×" Stands for the peak value of the related species.

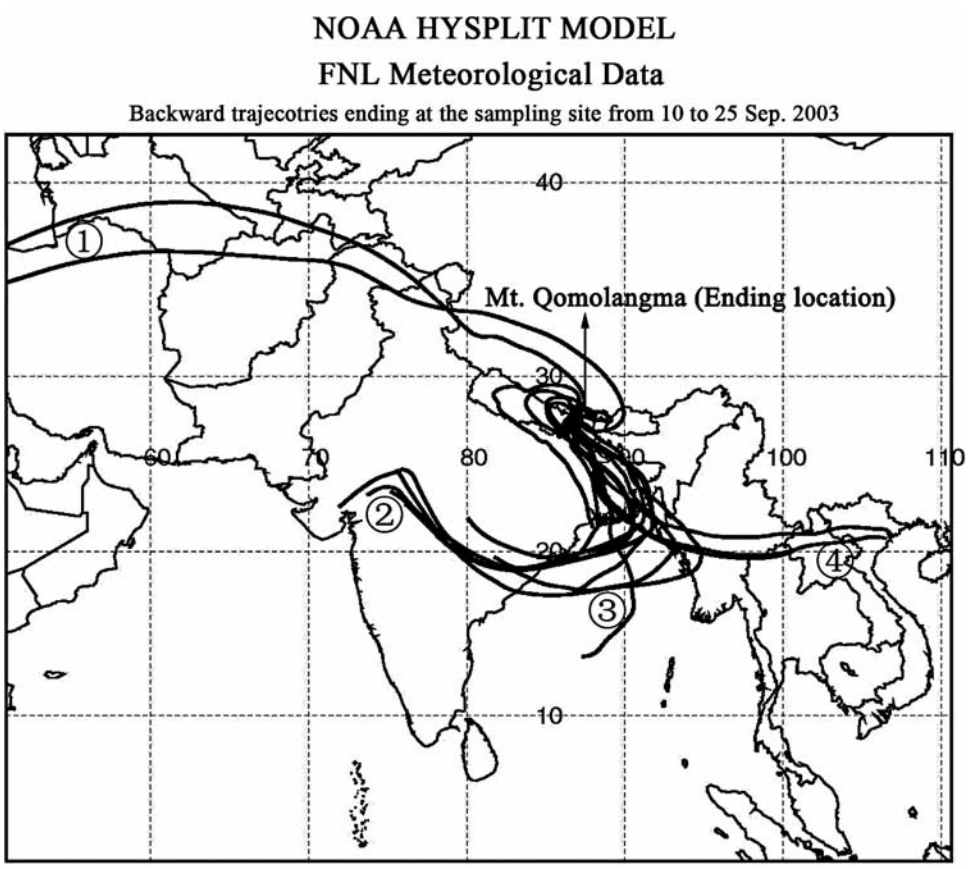

Figure 4. Categories of the 16 backward trajectories covering the experiment period.

at the isobaric layers of 600 and 700 hPa, except that the peak on 22/23 does not accord with the trend. We suggest that southerly air masses carried by monsoon dominate the Na^+ loading during our sampling period, except for the influence of westerly on 22/23. The sources of Na^+ were thought to have two main origins (marine aerosol or crustal dust) in some previous studies near Mt. Qomolangma [e.g., *Shrestha et al.*, 2002; *Kang et al.*, 2002a]. In the above context, we conclude that Ca^{2+} has dominantly continental desert sources. As showed in Table 2, the loading of Na^+ has four peaks during the sampling period, which are shown on 14/15, 16/17, 22/23, and 24/25, respectively. Thus we calculate Na^+/Ca^{2+} to identify the specific dominant air masses (marine or continental) for the related sampling time. The ratio of Na^+ and Ca^{2+} is included in Figure 7 (step plot). Apparently, on 14/15 and 22/23, the values of Na^+/Ca^{2+} do not present high but quite low even if Na^+ itself has fairly high loading in the filters, as Ca^{2+} shows high concentration caused by its desert sources during these time periods; while on 16/17, 17/18, 18/19, and 24/25, on the contrary, significant high Na^+/Ca^{2+} is shown in Figure 7. Hence we suggest continental air masses dominate the air quality of the sampling site on 14, 15, 22, and 23, while marine air masses dominate it on 16, 17, 18, 19, 24, and 25.

[24] Figure 8 presents a mean distribution of aerosol optical depth (AOD) in the area of 5–40°N, 60–110°E in September 2003. It is distinguishable that mean AOD over the India Subcontinent is generally higher than that over the Indian Ocean. And Figure 5 shows that all backward trajectories from 14 to 20 when SO_4^{2-} concentration peaks show are sourced from the continent of India and Southeast Asia other than from the ocean. Terra-MODIS and Aqua-MODIS data provide us the daily AOD values with the spatial resolution of $1 \times 1°$. We calculate the time-average AOD for each trajectory ending at our sampling site after matching each trajectory to related grids of $1 \times 1°$ it traverses, except the two ending on 22 and 23, which have very different transport pathways from the others. Figure 9 presents a comparison between SO_4^{2-} concentration and AOD for each trajectory. We can find that the variability of SO_4^{2-} and AOD has some rough consistency. Hence the conclusion could be drawn that maritime SO_4^{2-} has weak influence on the aerosol loading of our samples, and SO_4^{2-} could probably have the major source of continental emission. Recent studies [e.g., *Shrestha et al.*, 2000; *Kang et al.*, 2002a] suggest that SO_4^{2-} has various sources (anthropogenic or crustal) in atmosphere or glaciochemical records near Mt. Qomolangma. In our samples, SO_4^{2-} does not show simultaneous peaks with Ca^{2+} on 10/12 and 22/23 (Table 2; Figure 3), when Ca^{2+} is thought to have a significant crustal signal yet. Therefore crustal SO_4^{2-} from Central/West Asia or farther Africa could not contribute significantly to our samples on 10/12 and 22/23. As a certain area that most air trajectories must traverse, the Ganga basin is thought to have the major pollutant of sulfate aerosol due to growing anthropogenic activities [*Sharma et al.*, 2003]. It is natural

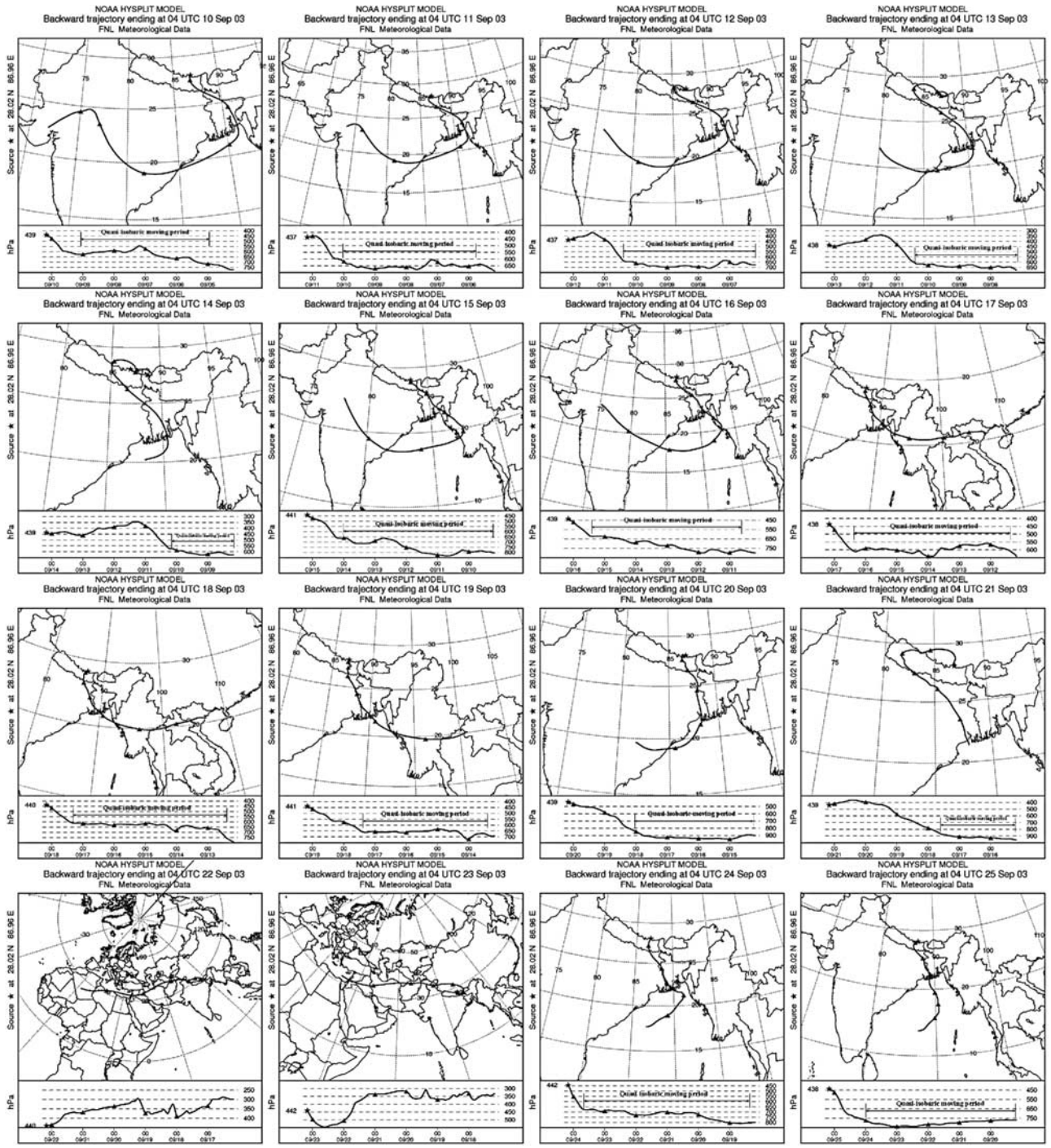

Figure 5. Daily backward trajectories ending at the sampling site.

to think that SO_4^{2-} in our samples has the major anthropogenic source. There are three concentration peaks of SO_4^{2-} in Table 2. The value of SO_4^{2-}/Ca^{2+} is calculated to separate anthropogenic source from dust source of the concentration peak of SO_4^{2-}. The value of SO_4^{2-}/Ca^{2+} is very low on 14/15 (Figure 10), when SO_4^{2-} and Ca^{2+} show simultaneous peaks of concentration (Figure 3). And two significant peaks show on 16/17 and 18/19. Thus SO_4^{2-} is suggested to have the major dust source on 14/15 and the major anthropogenic source on 16/17 and 18/19.

4.3. Fresh Snow Chemistry and Air-Snow Relationship

[25] During the field experiment, five fresh snow samples after each snowfall event were collected beside the aerosol sampling site. Although the total number of our snow samples is very limited, these samples facilitate comparison of overall trends in these two media. Figure 3 also presents the concentration of major ions of the fresh snow samples (black bars), and in general, they show a consistent variable pattern with those in aerosol samples.

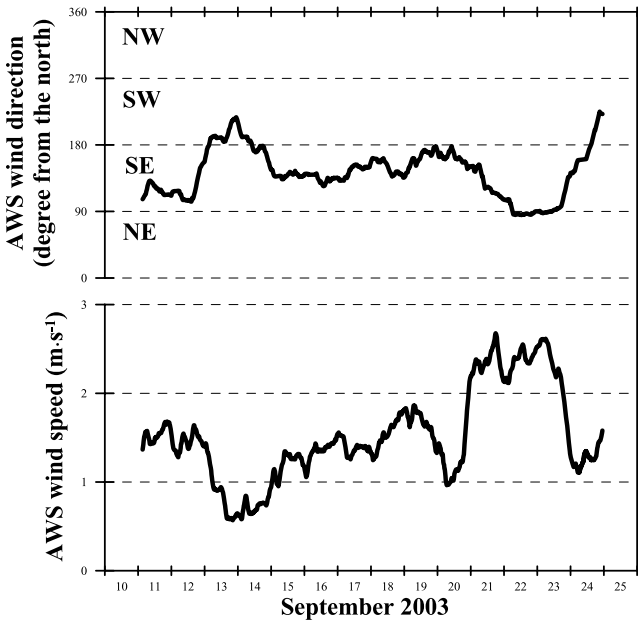

Figure 6. Local wind speed and wind direction recorded by AWS.

The concentrations of the species captured on 17 are all very low, possibly due to a heavy snowfall taking place on the night of 16.

[26] To investigate the air–snow relationship on the northern slope of Mt. Qomolangma which has not been studied before, scavenging ratios of the species in aerosol and fresh snow samples are calculated using snow and aerosol data according to the relationship $\omega = \rho_a \times C_s/C_a$, where ρ_a is air density (g m^{-3}) after correcting for the standard temperature and pressure; C_s is species concentration (ng g^{-1}) in fresh snow sample; and C_a is species concentration (ng m^{-3}) in the aerosol sample [*Davidson et al.*, 1993]. Mean values of scavenging ratios at Repula Col of East Rongbuk Glacier are compared to the results from previous studies done at other sites in Table 3.

[27] Because the limited number of our samples and light loading of most species with very large uncertainties except for SO_4^{2-} in our aerosol samples, Table 3 only presents a qualitative description of comparison. Scavenging ratios for K^+, Mg^{2+}, and Ca^{2+} in our samples are much higher than those in the previous studies (references in Table 3), and the ratios of Cl^- and NO_3^- are much lower than those at other sites, while the ratios of Na^+ and SO_4^{2-} are comparable to the others. It is noteworthy that corresponding ratios of these species on the south and north slopes of Mt. Qomolangma are very different. The ratios of the cations with farther distances from their sources on the north slope of Mt. Qomolangma are significantly bigger than those on the south slope, while the ratios of the anions with relatively closer sources on the south slope of Mt. Qomolangma are much bigger than those on the northern slope.

[28] Sulphate with the heaviest loading among the major ions on the northern slope of Mt. Qomolangma are much lower than that on the southern slope, which could be attributed to three factors: (1) it is the rainfall samples collected at Phortse, while snow samples were collected at Repula Col, and typically, the aerosol removal by snowfall is less efficient than that by rainfall and scavenging coefficient estimations are subject to more uncertainties due to the complex shapes of hydrometeors [*Scott*, 1982; *Pruppacher and Klett*, 1997; *Jennings*, 1998]; (2) the concentration of SO_4^{2-} on the north slope is significantly lower than that at Phortse, which means that cloud drops in air at the Repula Col have fewer chances to mix with the species than they do at Phortse; (3) the potential depletion occurs during transport since Phortse is closer to human activity area than Mt. Qomolangma.

[29] Scavenging ratio of SO_4^{2-} in this work is around 200, and this result is comparable to that in Greenland [*Davidson et al.*, 1985], maybe as the sampling sites of these two

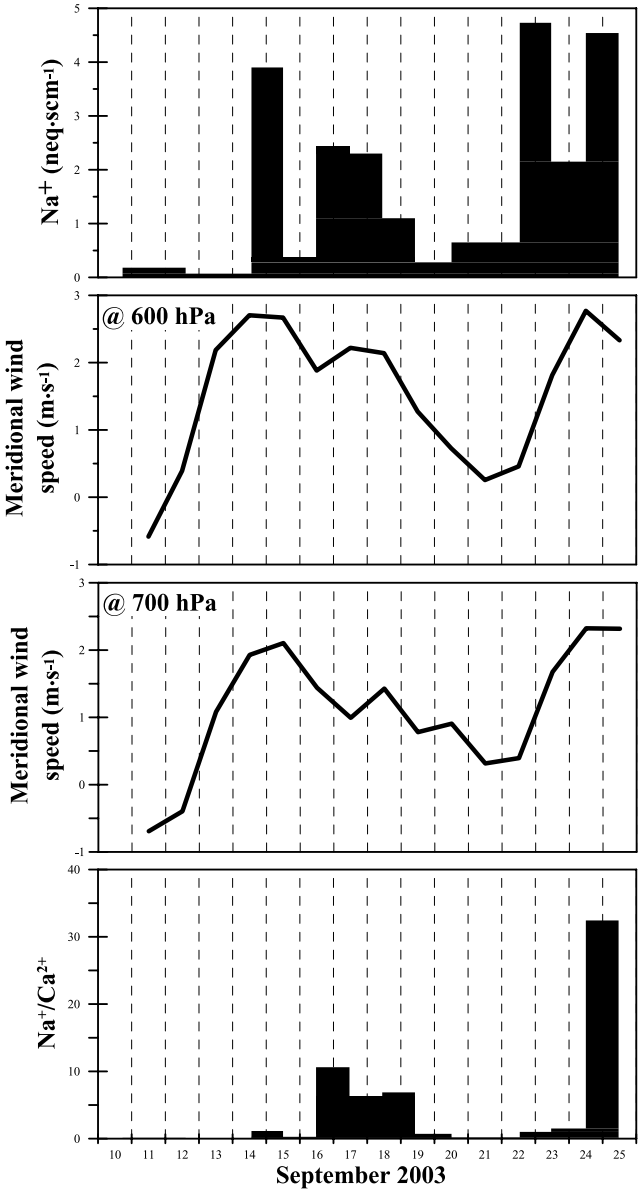

Figure 7. Concentration variations of Na^+, area-averaged meridional wind speed derived from the NCEP/NCAR reanalysis data at isobaric layers of 600 and 700 hPa, and time series of Na^+/Ca^{2+}.

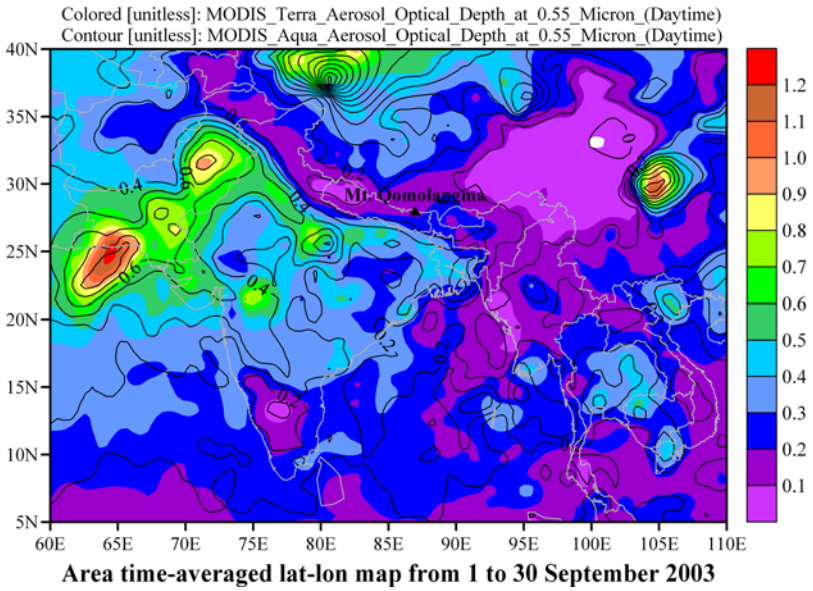

Figure 8. Time-averaged AOD map over the Indian Subcontinent in September of 2003.

works are both far remote sites, and both works are focused on the air–snow relationships.

5. Summary

[30] The investigations of aerosol chemistry and air–snow relationship are scarce at remote glacier sites. This work investigates the aerosol chemistry (including the species of Na^+, K^+, Mg^{2+}, Ca^{2+}, Cl^-, SO_4^{2-}, and NO_3^-) and air-snow relationship at Repula Col of East Rongbuk Glacier near Mt. Qomolangma during the late Indian summer monsoon season and is expected to be significant for improving on interpreting the detailed information in the massive debatable glaciochemical records here. During the sampling period, backward trajectory analysis shows air masses coming from the south and the west account for the air quality. The loading of anions are far heavier than that of cations, in which SO_4^{2-} accounts for nearly a half of the total loading. The relationship between some selected species concentration and their transport is discussed. Local emission by land weathering does not contribute significantly to the loading of Mg^{2+} and Ca^{2+}, and their high concentration is related to their continental desert sources. The meridional dynamic force of Indian monsoon is efficient to the loading of Na^+, and Na^+/Ca^{2+} could be used to distinguish air masses maritime or continental dominate the air quality. The signal of crustal SO_4^{2-} from Central/West Asia or farther Africa is weak, and mixed sources (anthropogenic and crustal) of SO_4^{2-} dominate its loading in aerosol samples. Air–snow scavenging ratios of these species are calculated and compared with the other results in some previous studies. The scavenging ratio of SO_4^{2-} as the most heavily loaded species is around 200, which is comparable with that in Greenland.

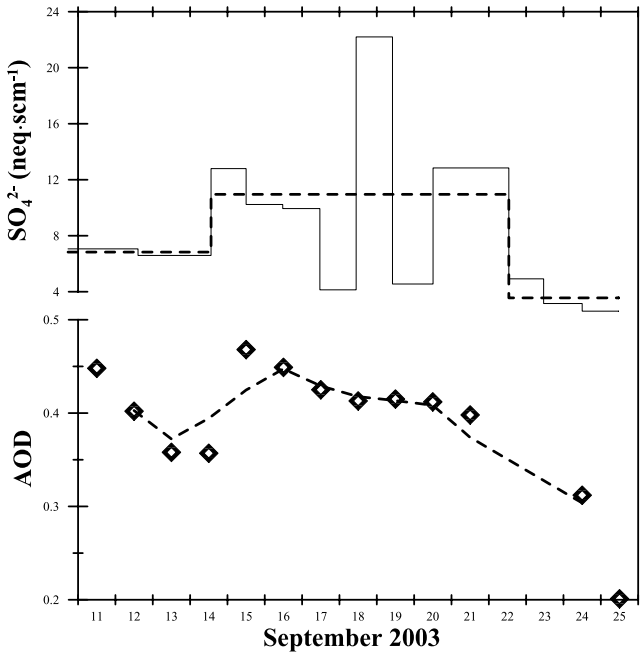

Figure 9. Comparison between SO_4^{2-} concentration and AOD of each trajectory.

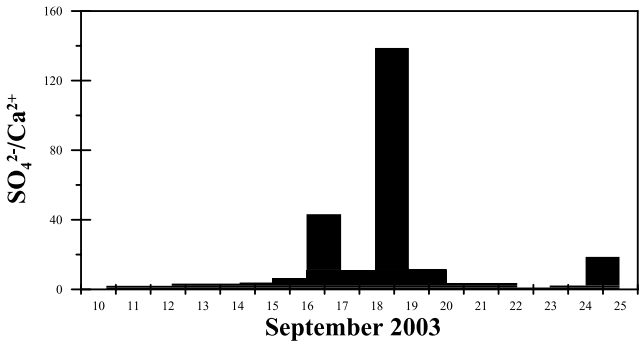

Figure 10. Time series of SO_4^{2-}/Ca^{2+}.

Table 3. Comparison of Air–Snow Scavenging Ratios at Different Sites

Items	Na^+	K^+	Mg^{2+}	Ca^{2+}	Cl^-	SO_4^{2-}	NO_3^-	Location	Reference
Mean	2202	3064	5880	4387	1280	202	417	Repula Col on the North Slope of Mt. Qomolangma	This Work
SD	2322	2484	4177	2279	2434	173	590		
Mean	2000	1200	1800	na	na	180	na	Dye 3, Greenland	*Davidson et al.* [1985]
SD	1200	620	1100	na	na	120	na		
Mean	na	na	na	2400	na	1000	na	Dye 3, Greenland	*Davidson et al.* [1993]
SD	na	na	na	na	na	na	na		
Mean	na	na	na	na	na	500	na	Summit, Greenland	*Silvente and Legrand* [1993]
SD	na	na	na	na	na	na	na		
Mean	na	na	na	na	na	350	940	Alpine Weissfluhjoch Davos Site, Switzerland	*Baltensperger et al.* [1993]
SD	na	na	na	na	na	na	na		
Mean	1880	1270	2680	2150	na	550	na	Glacier No. 1 at Headwater of Urumqi River, Mt. Tianshan, China	*Sun et al.* [1998]
SD	2200	930	2400	2170	na	140	na		
Mean	1393	2436	2580	1805	2582	487	2502	Phortse on the South Slope of Mt. Qomolangma	*Shrestha et al.* [2002]
SD	1593	2092	2277	1873	1870	326	2007		

"na" Stands for "not available".

[31] **Acknowledgments.** We would like to thank the reviewers, who have contributed valuable comments to improving the manuscript. Also we would thank all assistant members of the 2003 Glaciological Expedition of Mt. Qomolangma for their help in the field, X. Wang and J. Xu for their help to analyze the samples, J. Sun and C. Xiao for their suggestions on revising the manuscript. This work is supported by the National Nature Science Foundation of China (grants 40205007), the Social Commonweal Research Project of Ministry of Science and Technology of China (2005DIA3J106), and the "Talent Project" of Chinese Academy of Sciences.

References

Baltensperger, U., M. Schwikowski, H. W. Gaggeler, D. T. Jost, J. Beer, U. Siegenthaler, D. Wagenbach, H. J. Hoffmann, and H. A. Synal (1993), Transfer of atmospheric constituents into an Alpine snowfield, *Atmos. Environ.*, *27*, 1881–1890.

Davidson, C. I., S. Santhnam, B. C. Fortmann, and M. P. Olson (1985), Atmospheric transport and deposition of trace elements onto the Greenland ice sheet, *Atmos. Environ.*, *19*, 2065–2081.

Davidson, C. I., et al. (1993), Chemical constituents in the air and snow at Dye 3, Greenland: II. Analysis of Episodes in April 1989, *Atmos. Environ.*, *27*(A), 2723–2738.

Falkovich, A. H., E. Ganor, Z. Levin, P. Formenti, and Y. Rudich (2001), Chemical and mineralogical analysis of individual mineral dust particles, *J. Geophys. Res.*, *106*(D16), 18,029–18,036.

Goloub, P., J. L. Deuze, M. Herman, D. Tanre, I. Chiapello, B. Roger, and R. P. Singh (2001), Aerosol remote sensing over land using the spaceborne polarimeter POLDER, in *Current problems in atmospheric radiation*, edited by W. L. Smith and Y. M. Timofeyev, pp. 113–116, A. Deepak, Hampton, Va.

Hou, S., D. Qin, D. Zhang, S. Kang, P. A. Mayewski, and C. P. Wake (2003), A 154a high-resolution ammonium record from the Rongbuk Glacier, north slope of Mt. Qomolangma (Everest), Tibet–Himal region, *Atmos. Environ.*, *37*, 721–729.

Jennings, S. G. (1998), Wet Processes Affecting Atmospheric Aerosols, in *Atmospheric particles*, edited by R. M. Harrison and R. Van Grieken, pp. 476-507, John Wiley and Sons, New York.

Kahl, J. D. W., D. A. Martinez, H. Kuhns, C. I. Davidson, J. Jaffrezo, and J. M. Harris (1997), Air mass trajectories to Summit, Greenland: A 44-year climatology and some episodic events, *J. Geophys. Res.*, *102*(C12), 26,861–26,875.

Kang, S., D. Qin, P. A. Mayewski, C. P. Wake, and J. Ren (2001a), Climatic and environmental records from the Far East Rongbuk ice core. Mt. Qomolangma (Everest), *Episodes*, *24*(3), 176–181.

Kang, S., D. Qin, P. A. Mayewski, and C. P. Wake (2001b), 180 years $C_2O_4^{2-}$ records recovered from the ice core in Mt. Everest, some environmental implications, *J. Glaciol.*, *47*(156), 155–156.

Kang, S., P. A. Mayewski, D. Qin, Y. Yan, S. Hou, D. Zhang, J. Ren, and K. Kruetz (2002a), Glaciochemical records from a Mt. Everest ice core, relationship to atmospheric circulation over Asia, *Atmos. Environ.*, *36*(21), 3351–3361.

Kang, S., P. A. Mayewski, D. Qin, Y. Yan, D. Zhang, and S. Hou (2002b), Twentieth century increase of atmospheric ammonia recorded in Mt. Everest ice core, *J. Geophys. Res.*, *107*(D21), 4595, doi:10.1029/2001JD001413.

Kang, S., P. A. Mayewski, D. Qin, S. A. Sneed, J. Ren, and D. Zhang (2004), Seasonal differences in snow chemistry from the vicinity of Mt. Everest, central Himalayas, *Atmos. Environ.*, *38*, 2819–2829.

Langner, J., and H. Rodhe (1991), A global three-dimensional model of the tropospheric sulphur cycle, *J. Atmos. Chem.*, *13*, 255–263.

Legrand, M., and P. Mayewski (1997), Glaciochemistry of polar ice cores: A review, *Rev. Geophys.*, *35*, 219–243.

Liu, B. Y. H., D. Y. H. Pui, and K. L. Rubow (Eds.) (1984), Characteristics of air sampling filter media, in *Aerosols in the mining and industrial work environments*, edited by V. A. Maple and B. Y. H. Liu, pp. 989-1038, vol. 3, Instrumentation, Ann Arbor Science, (MI).

Marenco, F., et al. (2006), Characterization of atmospheric aerosols at Monte Cimone, Italy, during summer 2004: Source apportionment and transport mechanisms, *J. Geophys. Res.*, *111*, D24202, doi:10.1029/2006JD007145.

Marinoni, A., S. Polesello, C. Smiraglia, and S. Valsecchi (2001), Chemical composition of freshsnow samples from the southern slope of Mt. Everest region (Khumbu–Himal region, Nepal), *Atmos. Environ.*, *35*, 3183–3190.

Mayewski, P. A., W. B. Lyons, and N. Ahmad (1983), Chemical composition of a high altitude fresh snow fall in the Ladakh Himalayas, *Geophys. Res. Lett.*, *10*, 105–108.

Mayewski, P. A., M. J. Spencer, M. S. Twickler, and S. Whitlow (1990), A glaciochemical survey of the summit region, Greenland, *Ann. Glaciol.*, *14*, 186–190.

Nieuwolt, S. (1977), *Tropical climatology: An introduction to the climates of the low latitudes*, 207 p., John Wiley, New York.

Pruppacher, H. R., and J. D. Klett (1997), Microphysics of cloud and precipitation, 2nd ed., 954 p., Kluwer Academic Publishers, Dordrecht, Boston, London.

Qin, D., P. A. Mayewski, C. P. Wake, S. Kang, and J. Ren (2000), Evidence for recent climate change from ice cores in the central Himalayas, *Ann. Glaciol.*, *31*, 153–158.

Qin, D., S. Hou, D. Zhang, J. Ren, S. Kang, P. A. Mayewski, and C. P. Wake (2002), Preliminary results from the chemical records of an 80 m ice core recovered from the East Rongbuk Glacier, Mt. Qomolangma (Everest), *Ann. Glaciol.*, *35*, 278–284.

Ramachandran, S. (2005), PM2.5 mass concentrations in comparison with aerosol optical depths over the Arabian Sea and Indian Ocean during winter monsoon, *Atmos. Environ.*, *39*, 1879–1890.

Ramanathan, V., et al. (2001), Indian Ocean Experiment: An integrated analysis of the climate forcing and effects of the great Indo-Asian haze, *J. Geophys. Res.*, *106*(D22), 28,371–28,398.

Rasch, P. J., W. D. Collins, and B. E. Eaton (2001), Understanding the Indian Ocean Experiment (INDOEX) aerosol distributions with an aerosol assimilation, *J. Geophys. Res.*, *106*, 7337–7355.

Scott, B. C. (1982), Theoretical estimates of the scavenging coefficient for soluble aerosol particles as a function of precipitation type, rate and altitude, *Atmos. Environ.*, *16*, 1753–1762.

Sharma, M., Y. N. V. M. Kiran, and K. K. Shandilya (2003), Investigations into formation of atmospheric sulfate under high PM10 concentration, *Atmos. Environ.*, *37*, 2005–2013.

Shrestha, A. B., C. P. Wake, J. E. Dibb, P. A. Mayewski, S. I. Whitlow, G. R. Carmichael, and M. Ferm (2000), Seasonal variations in aerosol concentrations and compositions in the Nepal Himalaya, *Atmos. Environ.*, *34*, 3349–3363.

Shrestha, A. B., C. P. Wake, J. E. Dibb, P. A. Mayewski, and S. I. Whitlow (2002), Aerosol and precipitation chemistry at a remote Himalayan site in Nepal, *Aerosol Sci. Technol.*, *36*, 441–456.

Silvente, E., and M. Legrand (1993), Ammonium to sulphate ratio in aerosol and snow of Greenland and Antarctic regions, *Geophys. Res. Lett.*, *20*, 687–690.

Singh, R. P., S. Dey, S. N. Tripathi, V. Tare, and B. Holben (2004), Variability of aerosol parameters over Kanpur, northern India, *J. Geophys. Res.*, *109*, D23206, doi:10.1029/2004JD004966.

Sun, J., D. Qin, P. A. Mayewski, J. E. Dibb, S. Whitlow, Z. Li, and Q. Yang (1998), Soluble species in aerosol and snow and their relationship at Glacier 1, Tien Shan, China, *J. Geophys. Res.*, *103*(D21), 28,021–28,028.

Valsecchi, S., C. Smiraglia, G. Tartari, and S. Polesello (1999), Chemical composition of monsoon deposition in the Everest region, *The Science of the Total Environment*, *226*, 187–199.

Venkataraman, C., G. Habib, A. Eiguren-Fernandez, A. H. Miguel, and S. K. Friedlander (2005), Residential biofuels in South Asia: Carbonaceous aerosol emissions and climate impacts, *Science*, *307*, 1454–1456.

Wake, C. P., P. A. Mayewski, and M. J. Spencer (1990), A review of central Asian glaciochemical data, *Ann. Glaciol.*, *14*, 301–306.

Wake, C. P., J. E. Dibb, P. A. Mayewski, Z. Xie, Z. Li, P. Wang, and D. Qin (1994a), The chemical composition of aerosols over eastern Himalaya and Tibetan Plateau during low dust periods, *Atmos. Environ.*, *28*, 695–704.

Wake, C. P., P. A. Mayewski, Z. Li, J. Han, and D. Qin (1994b), Modern eolian dust deposition in central Asia, *Tellus*, *46*(B), 220–233.

Zhang, D., D. Qin, S. Hou, S. Kang, and J. Ren (2005), Climatic significance of (18O records from an 80.36 m ice core in the East Rongbuk Glacier, Mount Qomolangma (Everest), *Science in China (Series D)*, *48*(2), 266–272.

S. Kang, Institute of Tibetan Plateau Research, Chinese Academy of Sciences, Beijing 100085, China.

J. Ming, Institute of Geology and Geophysics, Chinese Academy of Sciences, Beijing 100029, China.

W. Tian, Zhengzhou Weather Modification Center, Chinese Meteorological Administration, Zhengzhou 450003, China.

D. Zhang, Institute of Climate System, Chinese Academy of Meteorological Sciences, 46 Zhongguancun Nandajie, Haidian District, Beijing 100081, China. (zhangdq@cams.cma.gov.cn)